Inorganic Chemistry
Article

Inorg. Chem. **2010**, *49*, 5377–5384 **5377**
DOI: 10.1021/ic100083b

Characterization of A New Copper(I)−Nitrito Complex That Evolves Nitric Oxide

Wan-Jung Chuang, I-Jung Lin, Hsing-Yin Chen, Yu-Lun Chang, and Sodio C. N. Hsu*

Department of Medicinal and Applied Chemistry and Center of Excellence for Environmental Medicine, Kaohsiung Medical University, Kaohsiung 807, Taiwan

Received October 29, 2009

The complexes [Cu(κ^2-$Ph_2PC_6H_4$(*o*-OMe))$_2$(CH_3CN)](BF_4) (**1**) and [CuCl($Ph_2PC_6H_4$(*o*-OMe))$_2$] (**2**) have been prepared by treating [Cu(CH_3CN)$_4$](BF_4) or CuCl with two equivalents *o*-(diphenylphosphino)anisole ($Ph_2PC_6H_4$-(*o*-OMe)) at room temperature, respectively. The reaction of **1** and (PPN)(NO_2) in acetonitrile solution affords a neutral compound [Cu($Ph_2PC_6H_4$(*o*-OMe))$_2$(ONO)] (**3**). In contrast to the synthesis of **3**, mixing $NaNO_2$ and **1** in MeOH yielded a unique dicopper(I) cationic species, [(($Ph_2PC_6H_4$(*o*-OMe))$_2$Cu)$_2$(μ-NO_2)]$^+$ (**4**) after ether/CH_2Cl_2 crystallization. The molecular structures of **1**−**4** have been determined by an X-ray diffraction study. The copper(I)−nitrito adduct **3** containing phosphine−ether ligands forms nitric oxide gas from the reaction with acetic acid, suggesting the first example and model compound in the asymmetric O-bound copper(I) nitrite intermediate microenvironment of copper nitrite reductases (Cu-NIRs).

Introduction

Copper-containing nitrite reductases (Cu-NIRs) active site contains a type I electron transfer center that is coupled via a His−Cys bridge to a type II catalytic center.[1−9] The reaction mechanisms of Cu-NIRs have been proposed on the basis of the results of numerous spectroscopic and crystallographic studies.[10−21] Those reaction mechanisms involve the formation of a copper(I)−nitro or −nitrito core species which forms from the reduction of oxidized Cu-NIRs, followed by nitrite binding or by binding of nitrite to oxidized Cu-NIRs followed by reduction. Recently, Soloman and co-workers suggested that the bidentate nitrito binding (O-bound) to copper is calculated to play a major role in the activating of the nitrite bond based on the density functional theory (DFT) calculated reaction coordinated for nitrite reduction in the reduced type II copper site.[20] The key challenge on the bioinorganic modeling area for a synthetic inorganic chemist is the synthesis of a copper(I)−nitro or −nitrito core adduct.

Nitrite anion may coordinate to a mononuclear copper cation in one of five ways, as demonstrated in Chart 1.[9,22] According to the hard−soft acid−base theory (HSAB), in the

*Corresponding author. E-mail: sodiohsu@kmu.edu.tw.

(1) Godden, J. W.; Turley, S.; Teller, D. C.; Adman, E. T.; Liu, M. Y.; Payne, W. J.; LeGall, J. *Science* **1991**, *253*, 438–442.
(2) Kukimoto, M.; Nishiyama, M.; Murphy, M. E. P.; Turley, S.; Adman, E. T.; Horinouchi, S.; Beppu, T. *Biochemistry* **1994**, *33*, 5246–5252.
(3) Suzuki, S.; Kohzuma, T.; Deligeer; Yamaguchi, K.; Nakamura, N. *J. Am. Chem. Soc.* **1994**, *116*, 11145–11146.
(4) Howes, B. D.; Abraham, Z. H. L.; Lowe, D. J.; Bruser, T.; Eady, R. R.; Smith, B. E. *Biochemistry* **1994**, *33*, 3171–3177.
(5) Averill, B. A. *Chem. Rev.* **1996**, *96*, 2951–2964.
(6) Suzuki, S.; Deligeer; Yamaguchi, K.; Kataoka, K.; Kobayashi, K.; Tagawa, S.; Kohzuma, T.; Shidara, S.; Iwasaki, H. *J. Biol. Inorg. Chem.* **1997**, *2*, 265–274.
(7) Farver, O.; Eady, R. R.; Abraham, Z. H. L.; Pecht, I. *FEBS Lett.* **1998**, *436*, 239–242.
(8) Suzuki, S.; Kataoka, K.; Yamaguchi, K. *Acc. Chem. Res.* **2000**, *33*, 728–735.
(9) Wasser, I. M.; de Vries, S.; Moenne-Loccoz, P.; Schroder, I.; Karlin, K. D. *Chem. Rev.* **2002**, *102*, 1201–1234.
(10) Hulse, C. L.; Averill, B. A. *J. Am. Chem. Soc.* **1989**, *111*, 2322–2323.
(11) Jackson, M. A.; Tiedje, J. M.; Averill, B. A. *FEBS Lett.* **1991**, *291*, 41–44.
(12) Ye, R. W.; Toro-Suarez, I.; Tiedje, J. M.; Averill, B. A. *J. Biol. Chem.* **1991**, *266*, 12848–12851.
(13) Murphy, M. E. P.; Turley, S.; Adman, E. T. *J. Biol. Chem.* **1997**, *272*, 28455–28460.
(14) Strange, R. W.; Murphy, L. M.; Dodd, F. E.; Abraham, Z. H. L.; Eady, R. R. *J. Mol. Biol.* **1999**, *287*, 1001–1009.
(15) Boulanger, M. J.; Kukimoto, M.; Nishiyama, M.; Horinouchi, S.; Murphy, M. E. P. *J. Biol. Chem.* **2000**, *275*, 23957–23964.
(16) Kataoka, K.; Furusawa, H.; Takagi, K.; Yamaguchi, K.; Suzuki, S. *J. Biochem.* **2000**, *127*, 345–350.
(17) Zhao, Y.; Lukoyanov, D. A.; Toropov, Y. V.; Wu, K.; Shapleigh, J. P.; Scholes, C. P. *Biochemistry* **2002**, *41*, 7464–7474.
(18) Antonyuk, S. V.; Strange, R. W.; Sawers, G.; Eady, R. R.; Hasnain, S. S. *Proc. Natl. Acad. Sci. U.S.A.* **2005**, *102*, 12041–12046.
(19) Tocheva, E. I.; Rosell, F. I.; Mauk, A. G.; Murphy, M. E. P. *Science* **2007**, *304*, 867–870.
(20) Ghosh, S.; Dey, A.; Sun, Y.; Scholes, C. P.; Solomon, E. I. *J. Am. Chem. Soc.* **2009**, *131*, 277–288.
(21) Nojiri, M.; Koteishi, H.; Nakagami, T.; Kobayashi, K.; Inoue, T.; Yamaguchi, K.; Suzuki, S. *Nature* **2009**, *462*, 117–120.
(22) Lehnert, N.; Cornelissen, U.; Neese, F.; Ono, T.; Noguchi, Y.; Okamoto, K.-i.; Fujisawa, K. *Inorg. Chem.* **2007**, *46*, 3916–3933.
(23) Halfen, J. A.; Mahapatra, S.; Olmstead, M. M.; Tolman, W. B. *J. Am. Chem. Soc.* **1994**, *116*, 2173–2174.
(24) Halfen, J. A.; Mahapatra, S.; Wilkinson, E. C.; Gengenbach, A. J.; Victor G. Young, J.; Lawrence Que, J.; Tolman, W. B. *J. Am. Chem. Soc.* **1996**, *118*, 763–776.
(25) Yokoyama, H.; Yamaguchi, K.; Sugimoto, M.; Suzuki, S. *Eur. J. Inorg. Chem.* **2005**, 1435–1441.
(26) Nairn, A. K.; Archibald, S. J.; Bhalla, R.; Boxwell, C. J.; Whitwood, A. C.; Walton, P. H. *Dalton Trans.* **2006**, 1790–1795.

Published on Web 05/19/2010

Chart 1. Bonding Modes of Copper−Nitrite and Copper−Nitrito Complexes

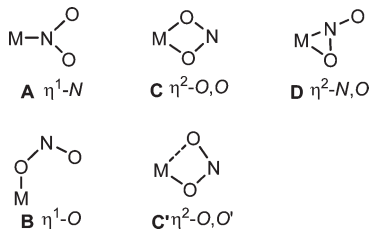

nitrite anion (NO_2^-), it should be expected that the soft Cu(I) cation would prefer N-bound (**A**; nitro),[23−27] while the harder Cu(II) cation would prefer O-bound in monodentate bonding mode (**B**; nitrito).[22,28−30] On the other hand, the binding of the nitrite anion in a bidentate fashion to a copper center would yield either an oxygen, O-bound species, η^2-*O*,*O* (**C**),[28,31−34] or a mixed nitrogen/oxygen-coordinated side on complex, η^2-*N*,*O* (**D**).[16,18] Additionally, the possibility of an asymmetric η^2-*O*,*O*′-bound moiety[35−37] (**C**′; similar to **C** or between **B** and **C**) containing only one formal Cu−O bond and a second "long-contact" Cu−O interaction (generally with a Cu−O length >2.5 Å) should also be considered. Bonding mode **D** may have not been reported in monocopper coordination chemistry but has been proposed in Cu-NIRs protein catalyzed cycles or observed in Cu-NIR protein crystallographic studies.[16,18] According to literature searching, nearly all of the known mononuclear Cu(II)-NO_2 compounds crystal structures contain an O-ligation nitrito moiety,[22,28−37] and the Cu(I)-NO_2 adducts are N-ligation nitrites.[23−27] An interesting solvent-induced interconversion between η^1-N-bound copper(II)−nitro and asymmetric O-bound copper(II)−nitrito bonding modes containing a tris(2-pyridylmethyl)-amine (TMPA) ligand was reported to show the possible nitrite-reduced intermediates in electrochemical reduction.[29] Regarding to copper(I)−nitro or −nitrito core species, there were only a few copper(I) nitrite coordination complexes that were characterized by a single crystal X-ray method.[23,25−27] Tolman and co-workers developed the first functional, mononuclear biomimetic model of Cu-NIRs, which is a nitro-bonding copper(I) complex [$L^{iPr3}Cu(NO_2)$] (L^{iPr3} = 1,4,7-triisopropyl-1,4,7-triazacyclononane) and its analogue binuclear complex $[(L^{iPr3}Cu)_2(\mu\text{-}NO_2)]^+$ as structural and functional models for the nitrite-binding type II copper site of Cu-NIRs.[23] Other researchers recently have proposed an intermediate from the spectroscopic titration of the copper(I)−nitro complex reduction process.[38] Recently, a series of copper(I)−nitro complexes modeling a system based on sterically hindered tris(1-pyrazolyl)methane and tris(4-imidazolyl)-carbinol ligands is reported and shows the steric and electronic effects of these tridentate ligands.[27] However, the copper(I)−nitrito (O-bound) complexes are seldom reported, only two known examples are the symmetric η^2-*O*,*O*-coordination on [$(PPh_3)_2$-$Cu(NO_2$-*O*,*O*)][39] and asymmetric η^2-*O*,*O*-coordination on [(2,6-(Ph_2P(*o*-C_6H_4)CH=N)$_2C_5H_3N$)$Cu(NO_2$-*O*,*O*′)],[40] which both contain the typical soft-base phosphine ligands. Reconsidering the bonding characteristic of copper nitrite bonding modes, it may not simply refer to the hard or soft ability of the local metal ion. The binding modes of nitrites may be influenced by the surrounding ligands environment of cooper(I) center. The phosphine ligands and nitrogen-donor ligands will provide different electronic properties to the copper(I) core that results in different NO_2-bonding behavior. To examine this thought, we chose another typical soft base *o*-(diphenylphosphino)anisole as a ligand environment to compare with other known type II copper(I)−nitro model complex containing aromatic and/or aliphatic nitrogen ligands,[23,25−27] which are classified into borderline bases and also compare with the only two known copper(I)−nitrito phosphine complexes [$(PPh_3)_2Cu(NO_2$-*O*,*O*)][39] and [(2,6-(Ph_2-P(*o*-C_6H_4)CH=N)$_2C_5H_3N$)$Cu(NO_2$-*O*,*O*′)],[40] the latter complex was reported very recently. In this paper, we report the synthesis and crystal structures of four copper(I) phosphine−ether ligand complexes with or without NO_2 bonding. The copper(I)−nitrito adduct [$Cu(Ph_2PC_6H_4$(*o*-OMe))$_2$(ONO)] (**3**) containing phosphine−ether ligands and possessing an asymmetric η^2-*O*,*O*′ bounded nitrito ligation (bonding mode C′) forms nitric oxide gas from the reaction with acetic acid, suggesting the first example and model compound in the asymmetric O-bound copper(I) nitrite intermediate microenvironment of copper nitrite reductases (Cu-NIRs).

Results and Discussion

Synthesis. The reaction of hemilabile phosphine−ether ligand[41,42] *o*-(diphenylphosphino)anisole ($Ph_2PC_6H_4$-(*o*-OMe)) with [$Cu(CH_3CN)_4$](BF_4) in CH_2Cl_2 under N_2 gives a copper(I) complex [$Cu(\kappa^2$-$Ph_2PC_6H_4$(*o*-OMe))$_2$-(CH_3CN)](BF_4) (**1**), which is isolated as a colorless solid. In the analogy to the preparation of **1**, we also examined the reaction of $Ph_2PC_6H_4$(*o*-OMe) ligand with CuCl to afford a neutral compound [$CuCl(Ph_2PC_6H_4$(*o*-OMe))$_2$] (**2**). Treatment of an acetonitrile solution of **2** with an equimolar amount of $AgBF_4$ under N_2 affords **1**, and a white precipitate silver chloride was formed as side product. The reaction of **1** and (PPN)(NO_2) in acetonitrile solution affords a colorless mononuclear neutral compound [$Cu(Ph_2PC_6H_4$(*o*-OMe))$_2$(ONO)] (**3**), which has an asymmetric η^2-*O*,*O*′ bounded nitrito ligation. In contrast to the synthesis of **3**, addition of $NaNO_2$ to a solution of **1** in MeOH yielded a yellow crystal after crystallization from ether/dichloromethane, which was characterized crystallographically as being a unique NO_2 bridge dicopper(I)

(27) Kujime, M.; Izumi, C.; Tomura, M.; Hada, M.; Fujii, H. *J. Am. Chem. Soc.* **2008**, *130*, 6088–6098.
(28) Hitchman, M. A.; Rowbottom, G. L. *Coord. Chem. Rev.* **1982**, *42*, 55–67.
(29) Komeda, N.; Nagao, H.; Kushi, Y.; Adachi, G.-y.; Suzuki, M.; Uehara, A.; Tanaka, K. *Bull. Chem. Soc. Jpn.* **1995**, *68*, 581–589.
(30) Beretta, M.; Bouwman, E.; Casella, L.; Douziech, B.; Driessen, W. L.; Gutierrez-Soto, L.; Monzani, E.; Reedjik, J. *Inorg. Chim. Acta* **2000**, *310*, 41–50.
(31) Tolman, W. B. *Inorg. Chem.* **1991**, *30*, 4877–4880.
(32) Ruggiero, C. E.; Carrier, S. M.; Tolman, W. B. *Angew. Chem., Int. Ed. Engl.* **1994**, *33*, 895–897.
(33) Casella, L.; Carugo, O.; Gullotti, M.; Doldi, S.; Frassoni, M. *Inorg. Chem.* **1996**, *35*, 1101–1113.
(34) Schneider, J. L.; Carrier, S. M.; Ruggiero, C. E.; Victor G. Young, J.; Tolman, W. B. *J. Am. Chem. Soc.* **1998**, *120*, 11408–11418.
(35) Walsh, A.; Walsh, B.; Murphy, B.; Hathaway, B. J.; *Acta Crystallogr.* **1981**, *B37*, 1512-1520 and references therein.
(36) Jiang, F.; Conry, R. R.; Bubacco, L.; Tyeklár, Z.; Jaeobson, R. R.; Karlin, K. D.; Peisach, J. *J. Am. Chem. Soc.* **1993**, *115*, 2095–2102.
(37) Stibraney, R. T.; Potenza, J. A.; Schugar, H. J. *Inorg. Chim. Acta* **1996**, *243*, 33–41.
(38) Kujime, M.; Fujii, H. *Angew. Chem., Int. Ed.* **2006**, *45*, 1089–1092.
(39) Halfen, J. A.; Tolman, W. B. *Acta Crystallogr.* **1995**, *C51*, 215–217.
(40) Chen, C.-S.; Yeh, W.-Y. *Chem. Commun.* **2010**, *46*, 3098–3100.
(41) Jeffrey, J. C.; Rauchfuss, T. B. *Inorg. Chem.* **1979**, *18*, 2658–2666.
(42) Hsu, S. C. N.; Hu, S.-C.; Wu, Z.-S.; Chiang, M. Y.; Hung, M.-Y. *J. Organomet. Chem.* **2009**, *694*, 1912–1917.

Scheme 1. Synthesis of Copper(I)−Phosphine Complexes with or without NO_2 Binding

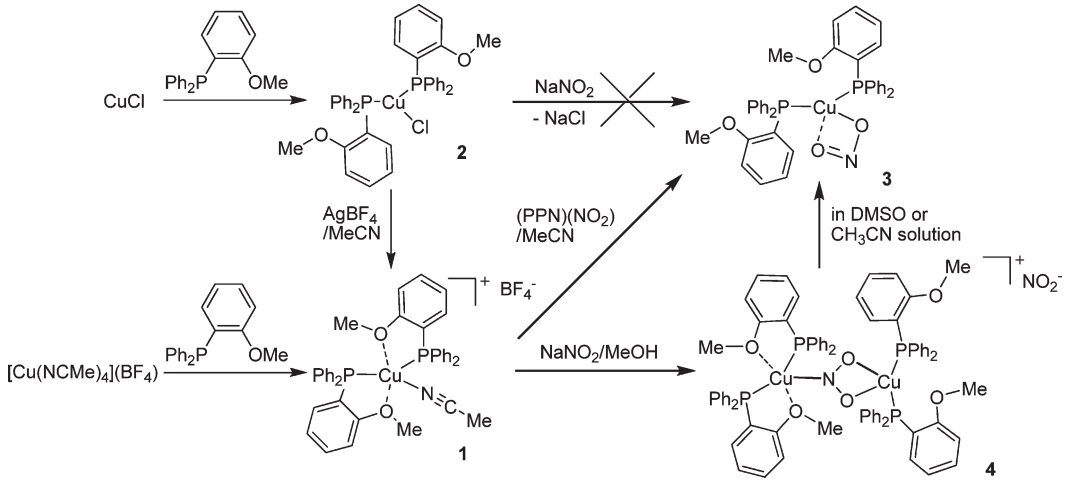

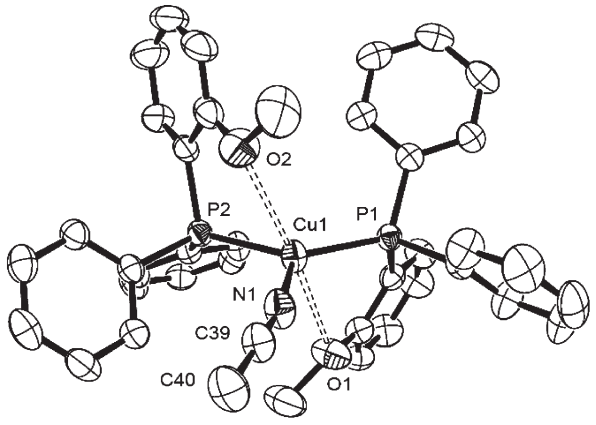

Figure 1. ORTEP representation of the molecular structure of **1** (50% ellipsoids, the hydrogen atoms are not shown, and the BF_4^- anion is artificially omitted for clarity).

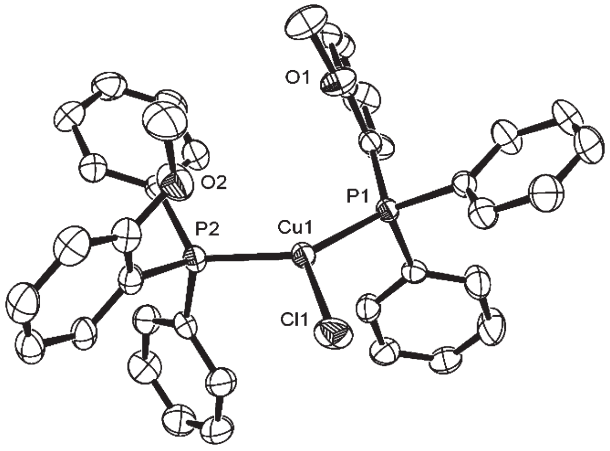

Figure 2. ORTEP representation of the molecular structure of **2** (50% ellipsoids and hydrogen atoms are not shown for clarity).

cationic species, $[((Ph_2PC_6H_4(o\text{-}OMe))_2Cu)_2(\mu\text{-}NO_2)]^+$ (**4**). To establish the formation of **4**, the recrystallization of **3** in ether/dichloromethane was also performed, which results **3** and did not convert to **4**. However, binuclear species **4** converts to **3** in acetonitrile or dimethyl sulfoxide (DMSO) solution. All reactions are summarized in Scheme 1.

X-ray Structural Investigations. Single crystals of **1** and **2** suitable for single crystal X-ray diffraction analysis were grown by laying a CH_3CN or CH_2Cl_2 solution of the compound with ether at 273 K, respectively. The crystallographic analysis structures of **1** and **2** are shown in Figures 1 and 2. Selected bond distances and angles of **1** and **2** are reported and compared in Table 1. Complexes **1** and **2** both contain two phosphine−ether ligands and afford a three-coordinated copper environment with coordinated CH_3CN or Cl. Previously, the importance of steric constraints in the related diphosphine−copper(I) complexes were well established,[43] so that the two $Ph_2PC_6H_4(o\text{-}OMe)$ ligands and coordinated CH_3CN or halide forming the trigonal complexes **1** and **2** are likely for steric reasons. The oxygen atoms of phosphine−ether ligands in **1** have short Cu···O contacts (Cu···O = 2.721 and 2.749 Å) that are less than the sum of the van der Waal radii (1.40(Cu) + 1.52 (O) = 2.92 Å) and may be considered as a dipole−ion interaction,[44] which are really different from **2**, while the nonbonded Cu···O distances of **2** are 3.349 and 3.525 Å. These features imply complex

Table 1. Selected Bond Lengths (Å) and Angles (°) for **1** and **2**[a]

	1	**2**
Cu(1)−P(1)	2.2223(7)	2.2326(6)
Cu(1)−P(2)	2.2449(8)	2.2387(6)
Cu(1)−N(1)	1.969(3)	
Cu(1)−Cl(1)		2.2240(7)
N(1)−C(39)	1.140(6)	
C(39)−C(40)	1.447(5)	
P(1)−Cu(1)−P(2)	129.12(3)	129.46(2)
P(1)−Cu(1)−N(1)	122.16(8)	
P(2)−Cu(1)−N(1)	108.538	
Cu(1)−N(1)−C(39)	166.7(3)	
P(1)−Cu(1)−Cl(1)		115.36(3)
P(2)−Cu(1)−Cl(1)		113.26(3)
Cu(1)···O(1)	2.721	3.349
Cu(1)···O(2)	2.749	3.525

[a] Estimated standard deviation is given in parentheses. Atoms are labeled as indicated in Figures 1 and 2.

(43) Bowmaker, G. A.; Engelhardt, L. M.; Healy, P. C.; Kildea, J. D.; Papasergio, R. I.; White, A. H. *Inorg. Chem.* **1987**, *26*, 3533–3538.

(44) Yeh, W.-Y.; Liu, Y.-C.; Peng, S.-M.; Lee, G.-H. *Inorg. Chim. Acta* **2005**, *358*, 1987–1992.

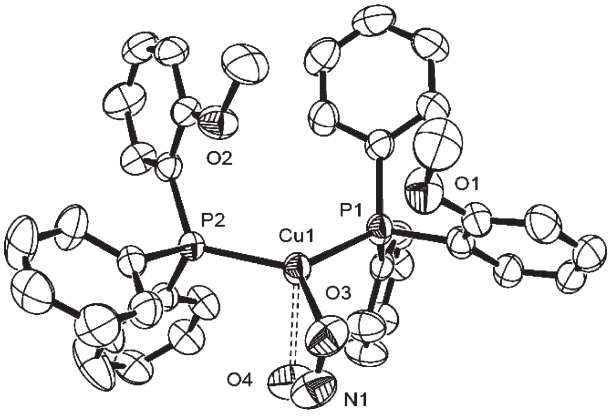

Figure 3. ORTEP representation of the molecular structure of **3** (50% ellipsoids, hydrogen atoms are not shown for clarity).

Table 2. Selected Bond Lengths (Å) and Angles (°) for **3** and **4**[a]

$Cu(Ph_2PC_6H_4(o\text{-}OMe))_2(ONO)$ (**3**)

Cu(1)−P(1)	2.2333(13)	Cu(1)−P(2)	2.2358(13)
Cu(1)−O(3)	2.116(4)	Cu(1)−O(4)	2.344(4)
N(1)−O(3)	1.227(6)	N(1)−O(4)	1.245(7)
P(1)−Cu(1)−P(2)	129.45(5)	P(1)−Cu(1)−O(3)	117.98(12)
P(2)−Cu(1)−O(3)	112.47(13)	O(3)−Cu(1)−O(4)	55.38(17)
O(3)−N(1)−O(4)	114.8(5)		

$[((Ph_2PC_6H_4(o\text{-}OMe))_2Cu)_2(\mu\text{-}NO_2)](NO_2)$ (**4**)

Cu(1)−P(1)	2.2241(16)	Cu(2)−P(2)	2.2249(17)
Cu(1)−N(1)	2.037(9)	Cu(1)···O(2)	2.924
Cu(2)−O(3)	2.230(6)	N(1)−O(3)	1.228(6)
P(1)−Cu(1)−P(1)^i	128.68(9)	P(2)−Cu(2)−P(2)^i	127.58(10)
P(1)−Cu(1)−N(1)	115.66(5)	O(3)−N(1)−O(3)^i	117.4(9)
O(3)−Cu(2)−O(3)^i	56.1(3)	O(3)−Cu(2)−P(2)	111.38(13)
O(3)−Cu(2)−P(2)^i	114.52(13)		

[a] Estimated standard deviation are given in parentheses. Atoms are labeled as indicated in Figures 3 and 4.

1 may be more reactive than **2** in the substitution reaction of $NaNO_2$. Indeed, the reaction of **1** with $(PPN)(NO_2)$ in acetonitrile solution leads to the substitution of an CH_3CN ligand of **1** to afford a colorless neutral compound $[Cu(Ph_2PC_6H_4(o\text{-}OMe))_2(ONO)]$ (**3**). On the other hand, complex **2** does not react with NO_2^- to form compound **3** at ambient temperatures.

Single crystals of **3** were grown by the diffusion of diethyl ether into an acetonitrile solution of the compound. The single crystal X-ray diffraction analysis shows the structure of **3** also consists of two phosphine−ether ligands and a novel O-bound nitrito ligand, in which an asymmetric η^2-*O*,*O*′-bound C′ bonding mode forms. The ORTEP drawing for the complex is depicted in Figure 3. Selected bond distances and angles of **3** are reported in Table 2. In contrast to the trigonal planar geometry in **1** and **2**, the copper atom of **3** is in a mildly distorted trigonal pyramidal environment with the Cu atom lying 0.087 Å above the plane (toward the O(4) atom) of the P(1), P(2), and O(3) atoms. A literature search of published data on Cu(I)−NO_2 complexes revealed that there were only two symmetric η^2-*O*,*O* bound moiety (bonding mode C) structures known, one featuring two PPh_3 ligand complexes $[(PPh_3)_2Cu(NO_2\text{-}O,O)]$ and another one that is a dicopper cationic species $[(L^{iPr3}Cu)_2(\mu\text{-}NO_2)]^{2+}$ (L^{iPr3} = 1,4,7-triisopropyl-1,4,7-triazacyclononane),[23,24,39] thus the asymmetric η^2-*O*,*O*′-bound moiety (bonding mode C′) here is a striking example of a neutral Cu(I)−nitrito complex bearing two phosphine−ether ligands. Particularly remarkable features of **3** have a wide P−Cu−P angle of 129.45(5)° and a smaller O−Cu−O angle of 55.38(17)° compared to related copper(I)−phosphine complexes, $[(PPh_3)_2Cu(NO_2\text{-}O,O)]$[39] (127.75(7)° and 56.7(2)°), which is more similar to the very recent example $[(2,6\text{-}(Ph_2P(o\text{-}C_6H_4)CH{=}N)_2C_5H_3N)Cu(NO_2\text{-}O,O')]$[40] (129.86(4)° and 56.7(2)°), respectively. The asymmetric nitrito-*O*,*O*′ coordinated with a Cu−O distance of 2.116(4) and 2.344(4) Å, which is significantly shorter and longer than the Cu(I)−$O_{nitrito}$ distance of the known copper(I) complexes $[(PPh_3)_2Cu(NO_2\text{-}O,O)]$[39] (2.191(4)Å) and $[(2,6\text{-}(Ph_2P(o\text{-}C_6H_4)CH{=}N)_2C_5H_3N)Cu(NO_2\text{-}O,O')]$[40] (2.131(4) and 2.197(4) Å), suggesting the asymmetric nitrito-*O*,*O*′ coordination leads to one Cu(I)−$O_{nitrito}$ interaction in **3** that is rather weak. The significant structural bonding mode difference of the known symmetric η^2-*O*,*O*-coordination of $[(PPh_3)_2Cu(NO_2\text{-}O,O)]$,[39] the slight asymmetric η^2-*O*,*O*′-coordination of $[(2,6\text{-}(Ph_2P(o\text{-}C_6H_4)CH{=}N)_2C_5H_3N)Cu(NO_2\text{-}O,O')]$[40] and **3** may derive from the more sterically hindered phosphine−ether ligand in **3** compared with other phosphine ligands.

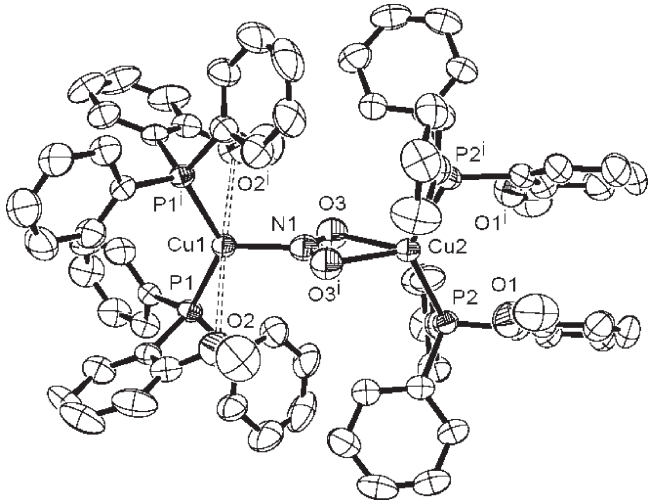

Figure 4. ORTEP representation of the molecular structure of **4** (50% ellipsoids, the hydrogen atoms are not shown, and the anion has artificially omitted for clarity).

An X-ray crystal structure determination confirmed the dimeric formulation for **4**, which represents a symmetric NO_2 bridge η^1-*N*; η^2-*O*,*O* dicopper cationic species $[((Ph_2PC_6H_4(o\text{-}OMe))_2Cu)_2(\mu\text{-}NO_2)]^+$ (**4**) with a nitrite counteranion. The ORTEP drawing for the complex **4** is depicted in Figure 4. Selected bond distances and angles of **4** are reported in Table 2. There is the molecular twofold rotational axis through Cu(1), N(1), and Cu(2). A tridentate bridging mode in which the NO_2^- ion is chelated to Cu(2) through two oxygen atoms and bridged to Cu(1) through nitrogen atom of nitrite anion. The coordination environment around Cu(1) of **4** is quite similar to that of **1**. The Cu(1)···O(2) contacts in **4** (2.924 Å) are almost equal to the sum of the van der Waal radii of copper and oxygen atoms, which may be better described as a consequence of packing constrains instead of bonding interaction. The coordination about the Cu(2) center

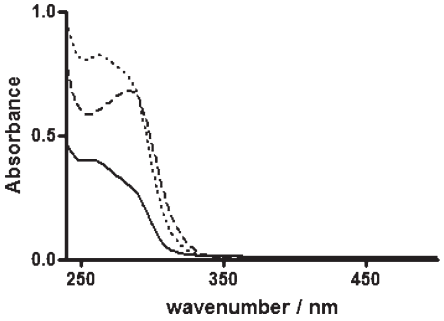

Figure 5. Electronic absorption spectra of **1** (solid line), **3** (dash line), and **4** (dotted line) in CH_2Cl_2 at room temperature.

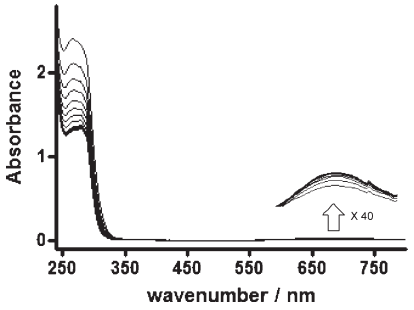

Figure 6. Spectral changes observed during the anaerobic reaction of **3** with acetic acid in CH_2Cl_2 at 298 K.

of **4** can be described as a distorted tetrahedral symmetry with a nitrito symmetric η^2-*O*,*O* bound moiety. The Cu(1)−$N_{nitrite}$ (2.037(9)Å) and Cu(2)−$O_{nitrito}$ (2.230(6)Å) distances in **4** are significantly longer than those of other related known copper(I) complexes containing such a bond, **3** (Cu−$O_{nitrito}$ = 2.116(4)Å), [L^{iPr3}Cu(NO_2)] (L^{iPr3} = 1,4,7-triisopropyl-1,4,7-triazacyclononane) (Cu−$N_{nitrite}$ = 1.903(2)Å),[23] [(L^{iPr3}Cu)$_2$(μ-NO_2)]$^{2+}$ (Cu−$N_{nitrite}$ = 1.899(2)Å and Cu−$O_{nitrito}$ = 1.968(2)Å),[24] and [(PPh_3)$_2$Cu(NO_2-*O*,*O*)] (Cu−$O_{nitrito}$ = 2.191(4)Å),[39] suggesting the bonding interactions between two copper and bridging nitrite anions in **4** are rather weak.

Spectral Characterizatons. The positive-ion electrospray mass spectra of **1**−**3** all gave a peak at m/z = 647, representing the parent ion with a loss of the coordinated CH_3CN, Cl^-, or NO_2^- ion from the metal. The dicopper(I) cationic species **4** can also confirm by positive-ion high-resolution electrospray mass specrum with a peak at m/z = 1342.3201 (Figures S1 and S2 in the Supporting Information). The relative abundances of its isotope patterns are in good agreement with those of a simulated one. The electronic absorption spectra of **1**−**4** in CH_2Cl_2 are shown in Figure 5 and Figure S3 in the Supporting Information. These copper(I)−phosphine complexes all give significant π−π* transition bands due to the phenyl groups of the phosphine ligands and have no absorption band in the visible region. Complexes **1** and **2** each exhibit intense broad bands around 258 and 288(sh) nm (for **1**) and 236 and 288 nm (for **2**), which could be assigned to MLCT transitions. Complexes **3** and **4** both also exhibit an intense broad band around 288 nm (for **3**), 264 and 288(sh) nm (for **4**), which is assigned to a Cu(I) → NO_2^- MLCT transition. Tolman et al. have reported that [L^{iPr3}Cu(NO_2)] (308 nm) and its analogue binuclear complex [(L^{iPr3}Cu)$_2$-(μ-NO_2)]$^+$ (338 and 380 nm) both exhibit intense metal-to-ligand charge transfer (MLCT) band(s) in CH_2Cl_2.[23] The shift of the MLCT band could be due to the different ligand electronic environments and NO_2 binding modes.

The DMSO-d_6 solution state $^{31}P\{^1H\}$ NMR spectrum of **1** and **2** both appears only as one broad singlet at δ −9.96 and −14.39, respectively, which is also consistent with the crystallographic results. In addition, the DMSO-d_6 (or CD_3CN) solution state $^{31}P\{^1H\}$ NMR of the yellow crystal **4** only shows one peak, which is similar with the $^{31}P\{^1H\}$ NMR of **3** in the same d-solvent (Figure S6 and S7 in the Supporting Information), which does not agree with the X-ray structure of **4**. This result may imply there is a solvent-induced transformation that occurs from **4** to **3**. By using CD_2Cl_2 as the d-solvent to investigate the solvent-induced behavior between **3** and **4**, it gives different results. In CD_2Cl_2, the $^{31}P\{^1H\}$ NMR spectrum (Figure S10 in the Supporting Information) of **4** has two peaks at δ −7.00 and −14.18 for the phosphine ligands, which are consistent with a C_2 symmetry in crystallographically results of **4**. In contrast, only one resonance (δ −14.85) appeared in the $^{31}P\{^1H\}$ NMR spectrum (Figure S10 in the Supporting Information) of **3**. The spectra of **3** and **4** in CD_2Cl_2 remain unchanged even in low temperature (223 K) $^{31}P\{^1H\}$ NMR experiments. Therefore, based on the synthesis observations and the spectroscopic results, they indicate that the solvent-induced formation of binuclear species **4** may attribute to different reaction solvents and suggest that a solvent-induced isomerization may happen when **4** converts to **3** in DMSO or MeCN solutions.

Reactivity with Acid and NO Generation. Previously, the best models for Cu-NIRs active site included the nitrite-bonding copper(I) complexes containing tridentate ligands; the nitrite is in the N-bound monodentate bonding mode (**A**).[23,25−27] In **3**, the microenvironment of an asymmetric η^2-*O*,*O*′-bound moiety to copper(I) is replicated and may react with acid to give nitric oxide. Therefore, the reactivity of **3** with a proton source was investigated. When six equivalents of acetic acid were added to a CH_2Cl_2 solution of **3** or **4** at room temperature, the color of the mixture solution changes from colorless to green-blue, and the evolution of NO gas (∼89 for **3** and ∼42% for **4**; see Table S1 in the Supporting Information) was identified by GC-TCD (Figure S12 in the Supporting Information) following the literature method.[23,25] According to the structure difference between **3** and **4**, the half NO generation yield for **4**, which is compared with **3**, may imply a catalyzing ability only on coordinated nitrites, not for the nitrite counterion. These results can be compared with the known copper(I)−nitro nitrogen ligand environment complexes (∼100 for [L^{iPr3}Cu(NO_2)][24] (L^{iPr3} = 1,4,7-triisopropyl-1,4,7-triazacyclononane); ∼95 for [Cu-(Me_2bpa)(NO_2)][25] (Me_2bpa = bis(6-methyl-2-pyridylmethyl)amine); and ∼70% for [(*i*Pr-TIC)Cu(NO_2)][27] (*i*Pr-TIC = tris(3,5-diisopropyl-1-pyrazoyl)methane) and indicate that the copper(I)−nitrito complexes with phosphine ligands (**3** and **4**) are also good functional Cu-NIRs models that produce known copper(II) acetate complexes and NO with acetic acid under anaerobic conditions. The known blue copper(II) product [$Cu_2(CH_3COO)_4(H_2O)_2$] was isolated from the NO generation reaction mixtures and demonstrated by crystallographic characterization.

The reaction of **3** with acetic acid was monitored by recording either the UV−vis absorption spectra at 5 min

Table 3. Rate Constants for the Nitrite Reduction of **3**[a]

temp(K)	$(10^5)k_{obs}$, $M^{-1}s^{-1}$
253	9.296 ± 0.16
273	40.34 ± 1.19
283	85.35 ± 1.59
298	217.0 ± 10.79

[a] The fit indicates $\Delta H^{\ddagger}$ of 40.89 (0.32) kJ mol^{-1} and $\Delta S^{\ddagger}$ −158.48 (1.18) J/K^{-1} mol^{-1} (numbers in parentheses indicate standard deviation).

intervals or the absorption vs time at a fixed wavelength (288 nm). At 298 K, the 288 nm band of **3** was observed to be a sharp peak, as shown in Figure 6. Adding acetic acid to the solution of **3** under N_2 induced a decrease in the absorbance at 288 nm and a slight increase in the absorbance at about 675 nm. The reaction of **3** with acetic acid was found to be first order both in [**3**] and in [acid]. This observation implies the rate-determining step only involves one protonation process. The temperature dependence of the rate of the reaction was examined at four temperatures over the range 253−298 K (Table 3). The analysis of these results using the usual Eyring approach (Figure S13 in the Supporting Information) gave $\Delta H^{\ddagger}$ of 40.89 ± 0.32 kJ mol^{-1} and $\Delta S^{\ddagger}$ of −158.48 ± 1.18 J/K^{-1} mol^{-1}. Comparison of the activation parameters for **3** and the known copper(I)−nitro complex [Cu(Me_2bpa)-(NO_2)][25] (Me_2bpa = bis(6-methyl-2-pyridylmethyl)amine; $\Delta H^{\ddagger}$ = 25 ± 1 kJ mol^{-1} and $\Delta S^{\ddagger}$ = −51 ± 3 J/K^{-1} mol^{-1}) reveals a significantly larger $\Delta H^{\ddagger}$ and a larger negative $\Delta S^{\ddagger}$ in the protonated process. Since a negative value of $\Delta S^{\ddagger}$ generally corresponds to the additional loss of freedom of motion by the solvating molecule, the larger negative $\Delta S^{\ddagger}$ value in **3** means a nearly complete protonation (association) process in the rate-determining step. This result may be attributable to the different ligand environment and coordination mode of NO_2. Therefore, the protonated **3** will be an active intermediate. The larger positive $\Delta H^{\ddagger}$ strongly suggests that **3** is more stable than protonated **3**.

Computational Results. Since the η^1-*N* or η^2-*O*,*O*′ bonding characteristic of copper nitrite bonding modes may not simply refer to the hard or soft ability of the local metal ion. It should be considered in the surrounding ligand environment of copper(I) center. Therefore, density functional theory (DFT) calculations have been performed to get insight into the bonding characteristic in complex **3**. The optimized geometry of bidentate η^2-*O*,*O*′ conformer of complex **3** is reasonably in agreement with the crystal structure (Table 2 and S2 in the Supporting Information); the average values of absolute deviation for bond length and angle are 0.049 Å and 3.3°, respectively.

Besides the η^2-*O*,*O*′ conformer, the calculations reveal that the monodentate η^1-*N* conformation is also a local minimum on the potential energy surface. However, the η^1-*N* conformer was found to be less stable than the η^2-*O*,*O*′ conformer by 3.07 and 3.69 kcal mol^{-1}, respectively, in terms of total electronic energy and free energy (Table S3 in the v), which is consistent with the observation that complex **3** crystallize in η^2-*O*,*O*′ bonding form. To further elucidate why the η^2-*O*,*O*′ bonding form is more stable than the η^1-*N* bonding form, the bonding energies between [Cu^+($Ph_2PC_6H_4$(*o*-OMe))$_2$] and nitrite were calculated and analyzed. It was found that the nitrite binds to [Cu^+($Ph_2PC_6H_4$(*o*-OMe))$_2$] more strongly in the η^2-*O*,*O*′ bonding mode (−117.60 kcal mol^{-1}) than in the η^1-*N* bonding mode (−112.41 kcal mol^{-1}), in line with the relative energies between the two conformers. These results can be compared with the known calculation results on the known copper(II)−nitrito complex [$TpCu^{II}$(η^2-NO_2-*O*,*O*)] (Tp = hydrotris(pyrazolyl)borate), which suggests the O-bound nitrito-bonding mode is favorable for the copper(II) case with the nitrogen-donor ligands.[22] Interestingly, the energy decomposition analysis, which partitions the bonding energy into physically meaningful terms of Pauli repulsion and electrostatic interaction as well as orbital interaction (including polarization and charge-transfer contributions), reveals that it is the smaller Pauli repulsion rather than electrostatic and orbital interactions accounting for the relatively larger stability for η^2-*O*,*O*′ conformation (Table S3 in the Supporting Information). The smaller Pauli repulsion in the η^2-*O*,*O*′ conformer relative to the η^1-*N* conformer is a consequence of the fact that the Cu···O contacts (2.185 and 2.316 Å) in the former are considerably longer than in the Cu···N contact (2.024 Å) in the latter (Table S3 in the Supporting Information).

To investigate the influences of phosphine−ether ligands on bonding between copper(I) and nitrite, we have carried out the corresponding calculations and analysis for the bare $Cu^+ \cdot NO_2^-$ complex. As observed in complex **3**, the bidendate O-bound configuration is more stable than the monodentate N-bound one; this can be, once again, attributed to the longer contact between copper and nitrite, which, in turn, leads to smaller Pauli repulsions in the η^2-*O*,*O*′ configuration than in the η^1-*N* configuration (Tables S2 and S3 in the Supporting Information). Although the phosphine−ether ligand does not alter the bonding mode of nitrite, the presence of it, however, significantly attenuates the bonding between nitrite and copper; the bonding energies decrease from −190.69 to −117.60 kcal mol^{-1} and from −187.73 to −112.41 kcal mol^{-1} for η^2-*O*,*O*′ and η^1-*N* configurations, respectively (Table S3 in the Supporting Information). The energy decomposition analysis clearly evidenced that the less attractive electrostatic interaction is responsible for the lowering of bonding energy caused by phosphine−ether ligands (Table S3 in the Supporting Information). This result is not surprising since a certain amount of electron transfer would occur from phosphine−ether ligands to copper(I) and, thus, reduces the effective positive charge on copper. As a result, the electrostatic stabilization between nitrite and copper would be smaller in complex **3** than in the bare $Cu^+ \cdot NO_2^-$.

Conclusion

The known type II copper(I)−NO_2 model complexes with aromatic and/or aliphatic nitrogen-donor ligands prefer to have a N-bound bonding mode.[23,25−27] However, nearly all of the crystal structures of the known mononuclear copper(II)−NO_2 complexes with similar nitrogen-donor ligand sets contain an O-bound conformation on the nitrite-bonding modes.[22,28−37] Since the binding modes of nitrite may be influenced by the surrounding ligand environment of the copper ion center. The nitrogen-donor ligands (hard or borderline bases) and phosphine ligands (soft base) would provide

different electronic environments around the copper ion core, which may induce dissimilar NO_2 bonding behavior. An O-bound copper(I)−nitrito complex **3** containing two phosphine−ether ligands has been prepared and revealed its asymmetric η^2-*O*,*O*′-bound moiety around the copper(I) atom by crystallographic analyses in this study. Phosphine−ether ligand ($Ph_2PC_6H_4$(*o*-OMe)) is a typical hemilabile ligand[41,42] which bonds to the copper(I) ion by the soft base side (phosphorus atom). Therefore, the phosphine ligands may induce the nitrite-bonding mode change from N-bound to O-bound on the copper(I) ion, which is significantly different from other known copper(I)−NO_2 complex containing nitrogen donor ligand sets. The DFT calculations also confirmed that the O-bound configuration is indeed more stable than the N-bound for $Ph_2PC_6H_4$(*o*-OMe) containing copper(I)−NO_2 complexes. Complex **3** is a striking example with significant asymmetric η^2-*O*,*O*′ nitrito structural-bonding mode for a recently conjectural biological Cu(I)−NO_2^- intermediate.[20] The protonation of **3** to release NO gas is of interest within the context of the chemistry of thoroughly examining the copper center of Cu-NIRs during the nitrite reduction process, which is important in order to enhance our understanding of the biological denitrification process.

Experimental Section

All manipulations were carried out under an atmosphere of purified dinitrogen with standard Schlenk techniques. Chemical reagents were purchased from Aldrich Chemical Co. Ltd., Lancaster Chemicals Ltd., or Fluka Ltd. All the reagents were used without further purification, apart from all solvents that were dried over Na (Et_2O, THF) or CaH_2 (CH_2Cl_2, CH_3CN) and then thoroughly degassed before use. The salt $[Cu(CH_3CN)_4](BF_4)$[45] and ligand $Ph_2PC_6H_4$(*o*-OMe)[41] were prepared as described in the literature. IR spectra were recorded on a Perkin-Elmer System 2000 FT-IR spectrometer. UV−vis spectra were recorded on an Agilent 8453 spectrophotometer. ^{1}H NMR, ^{13}C NMR, and ^{31}P NMR spectra were acquired on a Varian Gemini-200 proton/carbon FT NMR or a Varian Gemini-500 proton/carbon FT NMR spectrometer. ESI mass spectra were collected on a Waters ZQ 4000 mass spectrometer. Elemental analyses were performed on a Heraeus CHN-OS Rapid Elemental Analyzer. Gas chromatography thermal conductivity detector (GC-TCD) experiments were performed by using a Varian CP-3800 gas chromatography, Porpak Q column (6 ft, 20 mL/min flow rate, 30 °C, nitrogen carrier gas), and TCD detector.

[Cu(κ^2-$Ph_2PC_6H_4$(*o*-OMe))$_2$(CH_3CN)](BF_4) (1). A solution of $[Cu(CH_3CN)_4](BF_4)$ (0.100 g, 0.318 mmol) in CH_2Cl_2 (8 mL) was added dropwise to a stirring CH_2Cl_2 (15 mL) solution of $Ph_2PC_6H_4$(*o*-OMe) (0.185 g, 0.636 mmol). The reaction mixture was stirred overnight and concentrated to about 3 mL, then Et_2O (8 mL) was laying on the top and allowed to stay at room temperature for one day to obtain colorless crystals of [Cu(κ^2-$Ph_2PC_6H_4$(*o*-OMe))$_2$(CH_3CN)](BF_4) (**1**). Yield: 90% (0.225 g, 0.285 mmol). Anal. calcd for $C_{40}H_{37}O_2P_2NCuBF_4$: C, 61.91; H, 4.81; N, 1.80. Found: C, 61.77; H, 4.81; N, 1.95. ^{1}H NMR (DMSO-d_6): δ 2.07(s, 3H, CH_3CN), 3.41(s, 6H, −OCH_3), 6.69−7.53(m, 28H, Ph). ^{13}C{^{1}H} NMR (DMSO-d_6): δ 1.157(*C*H_3-CN), 55.58(O*C*H_3), 118.907(CH$_3$*C*N), 111.56−160.27(Ph). ^{31}P{^{1}H} NMR (DMSO-d_6): δ −9.96(s). UV−vis absorption (CH_2Cl_2, λ_{max}, nm)(ε/M^{-1}cm^{-1}) 230 (16 900), 258 (8500), 288sh (5900). ESI-MS: 647.08 (100%) [M−CH_3CN]$^+$.

[CuCl($Ph_2PC_6H_4$(*o*-OMe))$_2$] (2). A solution of CuCl (0.034 g, 0.343 mmol) in CH_3CN (10 mL) was added to a stirring CH_3CN (15 mL) solution of $Ph_2PC_6H_4$(*o*-OMe) (0.2 g, 0.686 mmol). A white solid precipitate forms immediately. The resulting white powder was recrystallized from CH_2Cl_2 to yield the product as colorless needles of [CuCl($Ph_2PC_6H_4$(*o*-OMe))$_2$] (**2**). Yield: 95% (0.223 g, 0.326 mmol). Anal. calcd for $C_{38}H_{34}ClCuO_2P_2$: C, 66.76; H, 5.01. Found: C, 66.77; H, 5.04. ^{1}H NMR (DMSO-d_6): δ 3.38-(s, 6H, −OCH_3), 6.69−7.53(m, 28H, Ph). ^{13}C{^{1}H} NMR (DMSO-d_6): δ 55.58(O*C*H$_3$), 120.95−169.95(Ph), 111.56−160.27(Ph). ^{31}P{^{1}H} NMR (DMSO-d_6): δ −14.39(s). UV−vis absorption (CH_2Cl_2, λ_{max}, nm)(ε/M^{-1}cm^{-1}) 236 (9600), 288 (6100). ESI-MS: 647.08 (100%) [M−Cl]$^+$.

[Cu($Ph_2PC_6H_4$(*o*-OMe))$_2$(ONO)] (3). A solution of **1** (0.2 g, 0.258 mmol) in CH_3CN (8 mL) was added to a stirring CH_3CN (7 mL) solution of (PPN)(NO_2) (0.151 g, 0.258 mmol). The resulting solution allowed staying at −20 °C for one day to obtain colorless crystals [Cu($Ph_2PC_6H_4$(*o*-OMe))$_2$(ONO)] (**3**). Yield: 75% (0.133 g, 0.193 mmol). Anal. calcd for $C_{38}H_{34}CuNO_4P_2$: C, 65.75; H, 4.94. Found: C, 65.72; H, 4.93. ^{1}H NMR (DMSO-d_6): δ 3.45(s, 6H, −OCH_3), 6.60−7.50(m, 28H, Ph). ^{13}C{^{1}H} NMR (DMSO-d_6): δ 55.59(O*C*H$_3$), 111.44−160.35(Ph). ^{31}P{^{1}H} NMR (DMSO-d_6): δ −13.00(s). ^{1}H NMR (CD_2Cl_2): δ 3.38(s, 6H, −OCH_3), 6.58−7.36(m, 28H, Ph). ^{31}P{^{1}H} NMR (CD_2Cl_2): δ −14.85(s). UV−vis absorption (CH_2Cl_2, λ_{max}, nm)(ε/M^{-1}cm^{-1}) 236 (18 400), 288 (14 300). FAB-MS: 647.13 [M−NO_2]$^+$. ESI-MS: 647.08 (100%) [M−NO_2]$^+$.

[(($Ph_2PC_6H_4$(*o*-OMe))$_2$Cu)$_2$(μ-NO_2)](NO_2) (4). A solution of **1** (0.7 g, 0.903 mmol) in MeOH (3 mL) was added to a stirring MeOH (18 mL) solution of $NaNO_2$ (0.0623 g, 0.903 mmol). The resultant mixture was stirred for 1 h to give a yellow solid precipitate, which was recrystallized from CH_2Cl_2/Et_2O to yield a yellow crystal product as [(($Ph_2PC_6H_4$(*o*-OMe))$_2$Cu)$_2$(μ-NO_2)]-(NO_2) (**4**). Yield: 86% (0.54 g, 0.402 mmol). ^{1}H NMR (DMSO-d_6): δ 3.30(s, 12H, −OCH_3), 6.45−7.45(m, 56H, Ph). ^{31}P{^{1}H} NMR (DMSO-d_6): δ −11.25. ^{1}H NMR (CD_2Cl_2): δ 3.32(s, br, 12H, −OCH_3), 6.38−7.65(m, br, 56H, Ph). ^{31}P{^{1}H} NMR (CD_2-Cl_2): δ −7.00 (s), −14.18(s). UV−vis absorption (CH_2Cl_2, λ_{max}, nm)(ε/M^{-1}cm^{-1}) 238 (21 800), 264 (17 500), 288sh (14 800). ESI-MS: 1342.03 (3%) [M−NO_2]$^+$, 939.03 (60%) [M−NO_2−Cu($Ph_2PC_6H_4$(*o*-OMe))]$^+$, 646.96 (100%) [M−NO_2−Cu(Ph_2P-C_6H_4(*o*-OMe))$_2$]$^+$. HRMS (ESI$^+$) *m*/*z* for $C_{76}H_{68}Cu_2NO_6P_4^+$ [M−NO_2]$^+$, calcd: 1342.2590. Found: 1342.2569.

Measurement of NO Generated from 3. A solution of **3** (33.3 mg, 0.048 mmol) in CH_2Cl_2 (0.9 mL) was prepared in a small vial capped with a rubber septum. A solution of acetic acid (10.8 μL) in CH_2Cl_2 (0.1 mL) was then introduced with a syringe at room temperature. The solution changed immediately from colorless to blue. Analysis of the headspace gas by a thermal conductivity detector indicated that NO had been generated (88.8 ± 1.6 for **3**). The NO generation data are obtained by five different experiments (see Table S1 and Figure S12, Supporting Information). NO concentration was performed by calibrating curve response with known concentrations of NO gas mixed with N_2 (120, 100, 80, 60,

(45) Kubas, G. J. *Inorg. Synth.* **1990**, *28*, 68–70.

(46) Frisch, M. J. T., G. W.; Schlegel, H. B.; Scuseria, G. E.; Robb, M. A.; Cheeseman, J. R.; Montgomery, J. A.; Vreven, T., Jr.; Kudin, K. N.; Burant, J. C.; Millam, J. M.; Iyengar, S. S.; Tomasi, J.; Barone, V.; Mennucci, B.; Cossi, M.; Scalmani, G.; Rega, N.; Petersson, G. A.; Nakatsuji, H.; Hada, M.; Ehara, M.; Toyota, K.; Fukuda, R.; Hasegawa, J.; Ishida, M.; Nakajima, T.; Honda, Y.; Kitao, O.; Nakai, H.; Klene, M.; Li, X.; Knox, J. E.; Hratchian, H. P.; Cross, J. B.; Bakken, V.; Adamo, C.; Jaramillo, J.; Gomperts, R.; Stratmann, R. E.; Yazyev, O.; Austin, A. J.; Cammi, R.; Pomelli, C.; Ochterski, J.; Ayala, P. Y.; Morokuma, K.; Voth, G. A.; Salvador, P.; Dannenberg, J. J.; Zakrzewski, V. G.; Dapprich, S.; Daniels, A. D.; Strain, M. C.; Farkas, O.; Malick, D. K.; Rabuck, A. D.; Raghavachari, K.; Foresman, J. B.; Ortiz, J. V.; Cui, Q.; Baboul, A. G.; Clifford, S.; Cioslowski, J.; Stefanov, B. B.; Liu, G.; Liashenko, A.; Piskorz, P.; Komaromi, I.; Martin, R. L.; Fox, D. J.; Keith, T.; Al-Laham, M. A.; Peng, C. Y.; Nanayakkara, A.; Challacombe, M.; Gill, P. M. W.; Johnson, B. G.; Chen, W.; Wong, M. W.; Gonzalez, C.; Pople, J. A.; *Gaussian 03,* , revision E, 1st ed.; Gaussian, Inc.: Wallingford, CT, 2004.

Table 4. Crystallographic Data for Complexes **1**- **4**

	1	**2**	**3**	**4**
empirical formula	$C_{40}H_{37}BCuF_4NO_2P_2$	$C_{38}H_{34}ClCuO_2P_2$	$C_{38}H_{34}Cu\ NO_4P_2$	$C_{76}H_{68}Cu_2N_2O_7P_4$
formula weight	776.00	683.58	694.14	1372.28
T (K)	200(2)	200(2)	200(2)	200(2)
cystal size (mm)	0.54 × 0.36 × 0.15	0.40 × 0.28 × 0.22	0.34 × 0.25 × 0.09	0.3 × 0.27 × 0.15
crystal system	triclinic	monoclinic	monoclinic	orthorhombic
space group	*P*-1	*C*2/*c*	*C*2/*c*	*Pncn*
a (Å)	10.7243(2)	22.2512(3)	22.2503(6)	18.0326(4)
b (Å)	13.0834(2)	16.0416(2)	15.9491(5)	20.1099(4)
c (Å)	14.5137(2)	19.2459(3)	19.8515(7)	20.5000(5)
α (°)	92.9650(10)	90	90	90
β (°)	97.8830(10)	105.1710(10)	105.5320(10)	90
γ (°)	107.9950(10)	90	90	90
V (Å^3)	1908.91(5)	6630.31(16)	6788.3(4)	7434.0(3)
Z	2	8	8	4
D_{calcd} (g cm^{-3})	1.350	1.370	1.358	1.226
μ mm^{-1}	0.710	0.869	0.779	0.709
reflns mcasd/indep	23 106/6655	20 951/5834	21 302/5957	38 987/6606
data/rcstraints/params	6655/0/462	5834/0/397	5957/0/415	6606/0/408
GOF	1.095	1.180	1.073	1.175
R_{int}	0.0463	0.0274	0.0812	0.0807
R_1 [$I > 2\sigma$] (all data)	0.0447 (0.1221)	0.0294 (0.0845)	0.0608 (0.1415)	0.0851(0.2434)
R_w [$I > 2\sigma$] (all data)	0.0575 (0.1351)	0.0407 (0.1034)	0.1083 (0.1718)	0.1367(0.2701)
max. pcak/hole (e$^-$/ Å^3)	0.903/−0.644	0.540/−0.681	0.522/−0.729	1.519/−2.213

and 40 ppm of NO in N_2); molar quantities were calculated using the ideal gas equation.

Kinetics. The kinetics studies of nitrite reduction of **3** in CH_2Cl_2 were carried out by monitoring the intensity decrease of the 288 nm band. The absorbance was detected by an Agilent 8453 spectrophotometer equipped with a custom-designed fiber-optics immersion quartz probe of 1 cm path length (Hellma) and fitted to a Schlenk flask containing 50 mL CH_2Cl_2 solution of **3** (8.7 mg, 0.25 mmol) under N_2 atmosphere. The reaction was started with the addition of 360 μL of acetic acid, which had been degassed with N_2 before use.

Computational methods. Geometry optimizations for complex **3** in η^2-*O*,*O*′ and η^1-*N* bonding modes were carried out at B3LYP/6-31+G* level. Vibrational frequency calculations were then performed to confirm that both optimized structures are local minima on the potential energy surface. These calculations were achieved by using the Gaussian 03 package.[46] The bonding energies between $Cu^{1+}(Ph_2PC_6H_4(o\text{-}OMe))_2$ and NO_2^- were evaluated by fragment orbital approach and analyzed by energy decomposition analysis implemented in ADF program.[47] In these calculations, B3LYP functional was used in combination with the basis sets of triple-ζ quality (TZP) and double-ζ quality (DZP) augmented by a set of polarization functions for copper and remaining elements, respectively.

X-ray crystal structure determinations. All X-ray reflections were measured with Mo Kα radiation (λ = 0.71073 Å) on a Nonius Kappa CCD diffractometer. The structures were solved with Direct Methods (program SHELXS-97). Refinement was performed with SHELXL-97 against F^2 of all reflections. Non-hydrogen atoms were refined with anisotropic displacement parameters. All hydrogen atoms were introduced in calculated positions and refined with a riding model. Geometry calculations and checking for higher symmetry was performed with the PLATON program. Further details are given in Table 4. The NO_2^- counterion and solvent molecule (diethylether, CH_2Cl_2) of **4** was disordered and in addition could not be completely located. All attempts to model satisfactorily this disorder were unsuccessful. Therefore, the disordered solvents were squeezed with the program PLATON prior to final refinement. The residual electron density in a two-fold symmetric unit was assigned to a whole NO_2^- counteranion.

Acknowledgment. Financial support of the National Science Council (Taiwan) and the Center of Excellence for Environmental Medicine in the KMU are highly appreciated. We thank Mr. Ting-Shen Kuo of National Taiwan Normal University for X-ray structural determinations and the National Center for High-Performance Computing for computer time and facilities.

Supporting Information Available: Text containing additional figures (Figure S1−S13), tables (Table S1−S3), and crystallographic data in CIF format for the structure determinations of **1**, **2**, **3** and **4**. These material are available free of charge via the Internet at http://pubs.acs.org.

(47) *ADF 2009.01*; SCM, Theoretical Chemistry Amsterdam, Vrije Universiteit: Amsterdam, The Netherlands, http://www.scm.com.